



Published in final edited form as:

*Nature*. 2020 April ; 580(7805): 621–627. doi:10.1038/s41586-020-2137-8.

## Late-stage oxidative C(sp<sup>3</sup>)–H methylation

Kaibo Feng<sup>†,1</sup>, Raundi E. Quevedo<sup>†,1</sup>, Jeffrey T. Kohrt<sup>2</sup>, Martins S. Oderinde<sup>3</sup>, Usa Reilly<sup>2</sup>, M. Christina White<sup>1</sup>

<sup>1</sup>Department of Chemistry, Roger Adams Laboratory, University of Illinois, Urbana, IL, USA

<sup>2</sup>Pfizer Worldwide Research and Development, Groton Laboratories, Eastern Point Road, Groton, Connecticut 06340, USA

<sup>3</sup>Research and Development, Bristol-Myers Squibb Company, Lawrenceville, NJ 08648, USA

### Summary Paragraph:

Frequently referred to as the “magic methyl effect”, installation of methyl groups, especially  $\alpha$  to heteroatoms, has been shown to drastically increase the potency of bioactive molecules<sup>1–3</sup>. Current methylation methods display limited scope and have not been demonstrated in complex settings<sup>1</sup>. Herein we report a regio- and chemoselective oxidative C(sp<sup>3</sup>)–H methylation method compatible with late-stage functionalization. A key to affecting this new chemistry was the combination of a highly site- and chemoselective C–H hydroxylation with a mild, functional group tolerant methylation. Using a small molecule manganese catalyst Mn(CF<sub>3</sub>PDP) at low loading (substrate/catalyst = 200) afforded targeted C–H hydroxylation on heterocyclic cores while preserving electron neutral and rich aryls. Fluorine or Lewis acid assisted formation of reactive iminium or oxonium intermediates enabled the use of a modestly nucleophilic organoaluminum methylating reagent that preserves other electrophilic functionalities on the substrate. The late-stage C(sp<sup>3</sup>)–H methylation is demonstrated on forty-one substrates housing sixteen different medicinally important cores incorporating electron-rich aryls, heterocycles, carbonyls, and amines. Eighteen pharmacologically relevant molecules with competing sites, including drugs (for example tedizolid) and natural products, are methylated site-selectively at the most electron rich, least sterically hindered position. Syntheses of two magic methyl substrates, an RORc inverse agonist and an S1P<sub>1</sub> antagonist, are demonstrated for the first time via late-stage methylation from the drug or its advanced precursor. Additionally, an unprecedented remote methylation of the B-ring carbocycle of an abiraterone analog is shown. The ability to methylate such complex molecules at late stages will reduce synthetic effort and thereby expedite broader exploration of the magic methyl effect in pursuit of novel small molecule therapeutics and chemical probes.

**Reprints and permissions information** is available at [www.nature.com/reprints](http://www.nature.com/reprints).

Correspondence and requests for materials should be addressed to M.C.W. (mcwhite7@illinois.edu).

<sup>†</sup>These authors contributed equally to this work.

**Author contributions** K.F. and R.E.Q. contributed equally by conducting the experiments and analyzing the data. M.C.W., K.F. and R.E.Q. wrote the manuscript. M.C.W., K.F., R.E.Q., J.T.K., M.S.O., U.R. designed the project. All authors provided comments on the experiments and manuscript during its preparation.

**Data availability** The data that support the findings of this study are available in the Supplementary Information and from the corresponding author upon reasonable request.

**Competing interests** The University of Illinois has filed a patent application on the Mn(CF<sub>3</sub>-PDP) catalyst.

Supplementary information is available in the online version of the paper.

The introduction of methyl groups has the potential to drastically improve the biological activities of a drug candidate by altering its binding affinity, solubility, and metabolism<sup>1–8</sup>. Such changes have been demonstrated to increase the potency of lead compounds up to more than 2000 folds and to enable interrogation of biological processes (Fig. 1a)<sup>6–8</sup>. Although methyl groups are ubiquitous in small-molecule drugs<sup>1</sup>, no general method is available to incorporate them in complex molecules at late stages. Accordingly, *de novo* synthesis, a rate-limiting step in drug discovery that impairs its overall atom-economy, is required<sup>9,10</sup>. A practical synthetic method that allows selective installation of methyl groups from C–H bonds at sites adjacent to heteroatoms, where the magic methyl effect is often most significant, would streamline diversification of drug leads and encourage more comprehensive investigations of this effect. Over the past decade, considerable progress has been made in developing C(sp<sup>3</sup>)–H alkylation methods where the *N*- or *O*-heterocycle acts as a nucleophilic coupling partner<sup>11–17</sup>. Such cross-couplings have shown broad scope with respect to alkyl electrophiles but limited scope of the metalated heterocyclic intermediates generated via substrate-controlled deprotonation or single-electron transfer (SET). Cases demonstrated with methyl electrophiles have focused on simple azacycles<sup>11,13,15–17</sup>. Expanding the heterocyclic scope to include dissymmetric substrates, epimerizable stereocenters, electrophilic functionalities (e.g., carbonyl, nitrile), remote basic amines, heteroaromatics, and halogenated aromatics remains a major challenge to be overcome for widespread use in late-stage diversification. Additionally, while direct C–C bond forming reactions may be desirable for installing larger and/or functionalized alkyl groups, direct methylation often results in inseparable mixtures with the starting material due to the methyl group's small size and electron neutrality.

We sought to approach C(sp<sup>3</sup>)–H methylation in *N*- and *O*-containing heterocycles in an oxidative fashion through a hydroxylated intermediate, with subsequent iminium or oxonium ion formation and methylation (Fig. 1b). Catalyst control could be leveraged to influence the site- and chemoselectivity of C–H hydroxylation in a broad range of heterocycles (Fig. 1c,d). Reports of alkylations of *N*-acyliminium ions are of limited scope<sup>18–20</sup>. Although C(sp<sup>3</sup>)–H oxidation  $\alpha$  to heteroatoms has been well-demonstrated, substrate-controlled selectivities can afford poor site- and chemoselectivity thereby limiting examples in complex settings. Additionally, the strong hyperconjugative activation of hemiaminals and hemiacetals typically promotes overoxidation to the corresponding carbonyl, calling for reduction prior to or after methylation (Fig. 1b)<sup>21–26</sup>.

The Mn(CF<sub>3</sub>PDP)(MeCN)<sub>2</sub>(SbF<sub>6</sub>)<sub>2</sub> **1** catalyst was reported to uniquely control site- and chemoselectivity in hydroxylating strong methylene C(sp<sup>3</sup>)–H bonds while tolerating halogenated arenes, although the tolerance for electron neutral or rich aromatic and some heteroaromatic rings remained a challenge (Fig. 1b)<sup>27</sup>. We questioned if sterically hindered catalyst **1** could result in faster C–H hydroxylation than alcohol oxidation for hyperconjugatively activated C–H bonds, and whether under milder oxidation conditions such a rate difference would increase chemoselectivity and yield for the hydroxylated product. Under the previously reported forcing conditions (10 mol% **1**, 5 equiv. H<sub>2</sub>O<sub>2</sub>)<sup>27</sup>, oxidation of arylated  $\gamma$ -lactam **2** afforded a significant amount of over-oxidation to the corresponding imide (Fig. 2a, **4b**, 41%). Lowering the catalyst and hydrogen peroxide



Alternative activation modes with AlMe<sub>3</sub> and methylating reagents with DAST were examined (Extended Data). In hemiaminals, base-mediated formation of an activated C–O bond (i.e., mesylation) gave predominantly elimination (Fig. 2a). Grignard reagents, even at cryogenic temperatures, afford diminished yields relative to AlMe<sub>3</sub>, likely due to poor functional group tolerance. Although ineffective for methylation of heterocyclic substrates, these reagents can be used to effect methylation in challenging linear secondary amine and carbocyclic substrates (*vide infra*, **51**, **53**).

We explored oxidative methylation for its capacity to methylate a collection of twenty-two compounds comprising ten different heterocyclic cores commonly found in pharmaceuticals (Fig. 3). A gram-scale methylation of **2** was successfully done in 71% yield via DAST activation; an ethyl group could also be installed using commercial triethylaluminum (**5**, 51%). Methylated  $\delta$ -lactam **6** was isolated in 58% yield; analogous to the  $\gamma$ -lactam, under more forcing oxidation conditions  $\delta$ -lactam gave predominantly imide (60%). For amide **2**, methylated **3** was observed in preparative yields with both DAST and BF<sub>3</sub> ionization (Fig. 2a). However, in oxazolidinones, housing more labile carbonyls, fluorination with DAST furnished significantly higher yields (**7**, 55% versus 10% with BF<sub>3</sub>, Extended Data; **8**, 63%). Pyrrolidine, the fifth most common nitrogen heterocycle in drugs<sup>35,36</sup>, undergoes hydroxylation with no significant over-oxidation to pyrrolidinone, followed by BF<sub>3</sub>-promoted methylation to afford mono-methylated product **9** in 54% yield. Critical for late-stage derivatization and orthogonal to most radical processes, high site-selectivity for methylation at the less sterically hindered methylene site was observed in substrates bearing more activated tertiary (3°) aliphatic, 3° benzylic, and 3°  $\alpha$ -carbonyl C–H bonds to afford products in preparative yields (**10–13**). Full stereoretention was measured with chiral substrates leading to **12** and **13**, indicating that the high regioselectivity is attributed to catalyst control of Mn(CF<sub>3</sub>PDP) **1** in the C–H cleavage step. Methyl ester, ketone, acetate, and nitrile, not well tolerated with strongly nucleophilic methylation reagents, were maintained using DAST activation/AlMe<sub>3</sub> methylation (**12–15**). Methylation on a 3-phenylpyrrolidine derivative proceeded regioselectively at the methylene site distal from the phenyl group, furnishing the 5-methylated product **16** in useful yield. Such chemoselectivity for electron neutral aromatics has not been previously demonstrated: at higher catalyst loadings, **1** afforded poor yields and chemoselectivities<sup>27</sup>.

In piperidines, the most common nitrogen heterocycle in small molecule drugs<sup>35,36</sup>, both DAST and BF<sub>3</sub> activation should be tried: enamine formation competes strongly with methylation and is highly dependent on both the substrate and the mode of hemiaminal activation (Fig. 3). For example, a piperidone derivative gave 2% of the methylated product with 60% enamine byproduct under DAST activation, whereas the BF<sub>3</sub> activation furnished **17** in 47% overall yield. Alternatively, methylation of piperidonyl-2-methyl acetate using BF<sub>3</sub> did not fully convert the hemiaminal to methylated product, whereas DAST activation afforded **18** in 64% yield. Gamma-substituted piperidines are prevalent structures in drugs, such as in paliperidone and paroxetine. An *N*-nosyl intermediate in the synthesis of paliperidone was selectively methylated using the DAST protocol to give **19** in 37% yield with no protection of the benzisoxazole ring  $\gamma$  to nitrogen. However, methylation of  $\gamma$ -(4-bromophenyl)piperidine with DAST resulted predominantly in enamine formation, while the

BF<sub>3</sub> activation strategy affording 39% yield of methylated **20**. Notably, all piperidines furnished a single observed methylated diastereomer, likely as a result of the rigid half-chair conformation of the iminium intermediate<sup>37</sup>.

Other simple cyclic amines, such as azepane, azabicycloheptane, and decahydroquinoline, were selectively methylated using the BF<sub>3</sub> activation protocol  $\alpha$ -*N* to afford 40%-46% overall yields of mono-methylated products **21-23**. Tetrahydroisoquinoline, among the top 20 nitrogen heterocycles in FDA-approved drugs<sup>36</sup>, was oxidatively methylated using BF<sub>3</sub> activation in good yields for both a brominated and an unsubstituted aromatic structure (**24**, 51%; **25**, 50%), with lower yields observed using DAST activation. In contrast to the majority of radical based oxidation methods that oxidize isochromans to isochromanones, under Mn(CF<sub>3</sub>PDP) **1** catalysis little over-oxidation is observed. 6,8-Dibromoisochroman was oxidatively methylated using DAST/AlMe<sub>3</sub> in 74% yield (**26**); BF<sub>3</sub> activation for these types of oxygen heterocycles afforded ring-opening products<sup>38</sup>.

We explored the ability of highly site- and chemoselective Mn(CF<sub>3</sub>PDP) **1** catalyzed C–H hydroxylation, coupled to a Lewis-acid/fluorine-promoted methylation, to provide a general method for installing methyl groups directly into the hydrocarbon cores of complex, bioactive molecules, thereby avoiding lengthy and costly *de novo* synthesis (Fig. 4)<sup>1,9,10</sup>. Cromakalim acetate, a potassium channel activator housing a  $\gamma$ -lactam with tertiary and secondary hyperconjugatively activated  $\alpha$ -NC(sp<sup>3</sup>)–H bonds, underwent oxidative methylation at the less activated but more sterically accessible secondary site in good yield (**27**, 51%). The acetate could be readily removed to furnish methylated cromakalim **28** in 85% yield. The methyl ester of indoprofen, an anti-inflammatory drug investigated for spinal muscular atrophy<sup>39</sup>, was oxidatively methylated at its central isoindolinone core in synthetically useful yields (**29**, 33%). The enhanced chemoselectivity of oxidative methylation with **1** under reduced loadings is evident when comparing with results at higher loadings (10 mol%), where **29** was obtained in diminished yields (7%) due to poor chemoselectivity. Chloroindoprofen methyl ester, a derivative with decreased electron density on the aromatic ring, undergoes oxidative methylation in higher yields (**30**, 55%). Fenspiride, an antitussive drug, was oxidatively methylated in a useful overall yield (**31**, 24%) at a methylene site adjacent to the quaternary center of an unprotected spiro-oxazolidinone, using (*S,S*)-Mn(PDP)(SbF<sub>6</sub>)<sub>2</sub> catalyst that is less sensitive to sterics<sup>27</sup>. The basic piperidine nitrogen of fenspiride was protected with HBF<sub>4</sub> and rendered a strong electron-withdrawing group, deactivating a distal benzylic site and three  $\alpha$ -*N* sites towards C–H oxidation<sup>40</sup>. Notably, SET reactions proceeding via basic amine catalysis (e.g. quinuclidine) are not amenable to this kind of nitrogen protection strategy and therefore do not undergo remote C–H functionalizations<sup>17,24</sup>. A derivative of pozanicline, a neuroprotective drug evaluated for ADHD treatment<sup>41</sup>, undergoes  $\alpha$ -*N* oxidative methylation at the pyrrolidine in useful yield and diastereoselectivity (**32**, 34%, 6:1 dr). The HBF<sub>4</sub> protection deactivates the basic pyridine moiety and its proximal ethereal sites from oxidation with **1**. While DAST activation produced similar yields, a higher diastereoselectivity was obtained with BF<sub>3</sub> activation (6:1 vs. 3:1), possibly due to different iminium counterions (Fig. 1b). The nosyl group on pyrrolidine, a convenient chromophoric protecting group for secondary amines, was readily removed using thiophenol and

subsequently protected with tert-butyloxycarbonyl (Boc) to afford **33** in 57% overall yield. Underscoring the unique chemoselectivity of this method, a derivative of the antidepressant diclofensine was oxidatively methylated at its tetrahydroisoquinoline core to afford **34** in useful yield despite the presence of a very electron rich methoxyphenyl. Mild, reductive desulfonation followed by reductive amination furnished Me-diclofensine **35** in 82% yield. The antidepressant drug citalopram, upon HBF<sub>4</sub> protection of the tertiary amine, is oxidatively methylated at its dihydroisobenzofuran core to afford **36**. DAST activation was used on the majority of these densely functionalized substrates whereas BF<sub>3</sub> activation was more effective on the tetrahydroisoquinoline core.

A precursor to pyrroloisoquinoline, a prevalent structure in compounds with neurotransmitter uptake inhibitor properties<sup>42</sup>, undergoes selective oxidative methylation at the less sterically hindered methylene site, versus the more activated tertiary, benzylic site, to furnish **37** (44% yield, Fig. 4a). Oxidation of a carbamate precursor to antibiotic tedizolid furnished substantial amounts of hemiaminal acetate that could be methylated in a useful overall yield under the TFAA/TMSOTf-assisted methylation (**38**, 44%). This method is operationally facile and can be performed on gram scale with no loss in efficiency (45% yield). Fluorination afforded lower yields of methylated product **38** due to unconverted hemiaminal acetate. The core piperidine of a paroxetine precursor and metabolite<sup>43</sup> was oxidatively methylated in useful overall yields (**39**, 34%) preferentially at the less sterically hindered methylene site remote from the 3-acetoxymethyl group. Nosyl deprotection and subsequent Boc protection afforded **40** in 86% yield. A piperidine derivative of the anti-inflammatory drug celecoxib was mono-methylated to afford **41** in good overall yield in the presence of an oxidatively labile tolyl group and pyrazole, both tolerated during C–H oxidation with **1** and requiring no protection. In these piperidine substrates, BF<sub>3</sub> activation was effective in furnishing methylated products.

Methylation of proline-based di-, tri-, and tetrapeptides proceeded with good overall yields and mass balances (**42**, **43**, **44**) with **1** under fluorine-assisted oxidative methylation conditions (Fig. 4a). Deoxo-Fluor may be used in substrates like tetrapeptide **44**, where isolation from the polar byproducts of DAST is challenging. Although effective in promoting arylation of peptides with electron rich aromatic nucleophiles, BF<sub>3</sub> activation in the AlMe<sub>3</sub> methylation of peptides afforded complex mixtures, likely arising from activation of the amide carbonyls<sup>30</sup>. Ambroxide, a naturally occurring terpenoid, also undergoes selective oxidative methylation using DAST at a methylene site  $\alpha$  to oxygen on its tetrahydrofuran ring to afford **45** in 32% yield (with 19% of sclareolide lactone). The use of BF<sub>3</sub> in this case promoted ring-opening. Significantly, Fe(PDP), ruthenium-mediated oxidation, and **1** under forcing conditions all afforded sclareolide lactone as the major product isolated (see SI)<sup>10,21,28</sup>.

The sultam ring in an advanced intermediate of an RORc inverse agonist **46** (Fig. 4b) was oxidatively methylated with **1** using TFAA/TMSOTf activation/AlMe<sub>3</sub> to afford **47** as the *syn*-diastereomer. Other activation modes, such as BF<sub>3</sub>, resulted in deleterious elimination pathways. Notably, an oxidatively labile phenyl moiety and a doubly activated benzylic methylene site were tolerated. Previous installation of the *syn*-methyl group afforded a 13-fold increase in RORc SRC1 selectivity relative to the unmethylated version; however, it

required a six-step *de novo* synthesis proceeding in 1.4% overall yield<sup>5</sup>. This analog and others are now accessible via cross-coupling with methylated intermediate **47**.

Tedizolid, a commercial oxazolidinone antibiotic for acute bacterial skin infections, bears numerous oxidatively sensitive functional groups such as a pyridine, tetrazole, and an *N*-methyl (Fig. 4c). Mn(CF<sub>3</sub>PDP) **1** oxidation (2 mol%) of tedizolid acetate **48** proceeded in *ca.* 53% yield of oxidized products (3:1 hemiaminal/acetate) with no protection of the dense nitrogen functionalities. The significant challenge was to identify a procedure to install the methyl group from the hemiaminal intermediates. Activation via fluorination furnished primarily eliminated products not observed on the simpler core structure (**38**, Fig. 4a), while BF<sub>3</sub> activation resulted in side reactions. However, under TFAA/TMSOTf activation, elimination was suppressed and the methylated product **49** was obtained in a remarkable 40% overall yield, 74% per step, comparable to that of the simpler precursor **38**. Deprotection of the acetate in 92% yield afforded Me-tedizolid **50**, an interesting candidate for future biological evaluation given that a 9-fold boost in potency has been reported for similar oxazolidinone cores with methylation at the same position (Fig. 1a)<sup>44</sup>.

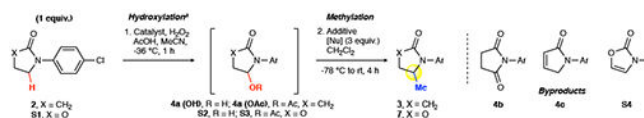
We questioned if the scope of this reaction could be extended beyond heterocycles, and found that oxidative C–H methylation is not restricted to substrates that can form iminium or oxonium intermediates: promising reactivity has been observed for both imines and remote alcohols generated via C–H hydroxylation with **1**. An S1P<sub>1</sub> antagonist, whose benzylic and aromatic methylations afforded a 2135-fold potency increase<sup>6</sup>, was methylated in its methyl ester form (**51**, Fig. 4d). While oxidation of the antagonist was successful without need for protection of the aniline motif, the resulting imine was much less reactive than an iminium and required a stronger nucleophile than AlMe<sub>3</sub>. In this case, we found that methylmagnesium bromide at cryogenic temperatures, with TMSOTf activation of the imine, produced the methylated product without eroding the amide and ester functional groups (**52**, 14%, 52% per step).

At higher catalyst loadings, Mn(CF<sub>3</sub>PDP) **1** is an effective catalyst for methylene C–H bond hydroxylations<sup>27</sup>. Abiraterone analog **53** was hydroxylated in *ca.* 32% yield (with 16% ketone) in one step, without recycling the starting material as required in Fe(CF<sub>3</sub>PDP) catalysis (Fig. 4e)<sup>40</sup>. In carbocyclic substrates, displacement of a C–F bond or ionization with a Lewis acid is difficult; however, mesylates of such aliphatic alcohols are stable and can be activated by AlMe<sub>3</sub> to undergo substitution<sup>45</sup>. By replacing fluorination with mesylation, **53** was successfully methylated as a single observed diastereomer (**54**, 15% overall yield, 53% per step), likely through a carbocation intermediate. To the best of our knowledge, this is the first method that enables such remote methylation at unactivated C(sp<sup>3</sup>)–H bonds. The discovery of this reactivity underscores the importance of developing methylene oxidations that afford predominately alcohol products.

## Extended Data

Extended Data Table 1 |

Reaction Optimization.



Entry	Substr.	Catalyst	Loading (mol%)	Additive	[Nu]	4a (OH)/S2 (%)	4a (OAc)/S3 (%)	3/7 (%)	4b (%)	4c/S4 (%)	rsm (%)
<b>Oxidation</b>											
1 <sup>b</sup>	2	Fe(PDP)	3 x 5	-	-	<5 <sup>k</sup>	0	-	<5 <sup>k</sup>	-	0
2 <sup>c</sup>	2	Fe(CF <sub>3</sub> PDP)	3 x 5	-	-	8 <sup>k</sup>	0	-	6 <sup>k</sup>	-	0
3 <sup>d</sup>	2	Mn(PDP) (OTf) <sub>2</sub>	1	-	-	12	0	-	0	-	75
4	2	Mn(PDP) (SbF <sub>6</sub> ) <sub>2</sub>	1	-	-	28	7	-	<5 <sup>k</sup>	-	35
5 <sup>e</sup>	2	Mn(CF <sub>3</sub> PDP) 1	10	-	-	13 <sup>k</sup>	10	-	41	-	0
6	2	1	1	-	-	51	21	-	9	-	0
7	2	1	0.5	-	-	64	18	-	<5 <sup>k</sup>	-	4
<b>Methylation</b>											
8 <sup>f</sup>	2	1	0.5	BF <sub>3</sub> •OEt <sub>2</sub>	AlMe <sub>3</sub>	<5 <sup>k</sup>	0	63	<5 <sup>k</sup>	0	11
9 <sup>f</sup>	S1	1	0.5	BF <sub>3</sub> •OEt <sub>2</sub>	AlMe <sub>3</sub>	11	5	10	-	4	27
10 <sup>g</sup>	S1	1	0.5	DAST	AlMe <sub>3</sub>	0	14 <sup>k</sup>	55	-	0	16
11 <sup>g</sup>	2	1	0.5	DAST	AlMe <sub>3</sub>	0	0	64	<5 <sup>k</sup>	0	12
12 <sup>g</sup>	2	1	0.5	Deoxo-Fluor	AlMe <sub>3</sub>	0	0	61	6	0	5
13 <sup>h</sup>	2	1	0.5	TFAA/TMSOTf	AlMe <sub>3</sub>	0	0	51	<5 <sup>k</sup>	14	9
14 <sup>h</sup>	S1	1	0.5	TFAA/TMSOTf	AlMe <sub>3</sub>	0	0	46	-	20	13
15 <sup>i</sup>	2	1	0.5	MsCl/Et <sub>3</sub> N	AlMe <sub>3</sub>	15	0	0	<5 <sup>k</sup>	39	6
16 <sup>g</sup>	2	1	0.5	DAST	ZnMe <sub>2</sub>	17	9	0	11	0	14
17 <sup>g,j</sup>	2	1	0.5	DAST	MeMgBr	24	<5 <sup>k</sup>	24	<5 <sup>k</sup>	0	9

<sup>a</sup> General oxidation (unless otherwise noted): 2 (0.3 mmol), catalyst (x mol%, (*R,R*) and (*S,S*) used interchangeably), AcOH (15 equiv.), MeCN (0.5 M), -36 °C; H<sub>2</sub>O<sub>2</sub> (2 equiv.) in MeCN (3.75 mL) syringe pump 1 h. Mixture passed through silica plug, EtOAc flush, concentrated prior to isolation or methylation. Isolated product yields.

<sup>b</sup> Procedure ref. 28.

<sup>c</sup> Procedure ref. 29.

<sup>d</sup> Procedure ref. 31.

<sup>e</sup> 5 equiv. H<sub>2</sub>O<sub>2</sub>.

<sup>f</sup> General BF<sub>3</sub> alkylation: crude in CH<sub>2</sub>Cl<sub>2</sub> (0.2 M), -78 °C, AlMe<sub>3</sub> (3 equiv.) and BF<sub>3</sub>•OEt<sub>2</sub> (2 equiv.) sequentially added, stirred 1 h; room temperature (rt) for 3 h.



<sup>g</sup>General fluorine alkylation: crude in CH<sub>2</sub>Cl<sub>2</sub> (0.2 M), fluorine additive (1 equiv.) added at –78 °C; rt for 1 h; cooled to –78 °C, nucleophile (3 equiv.) added, stirred 2 h; rt for 1 h.

<sup>h</sup>General TMSOTf alkylation: crude in CH<sub>2</sub>Cl<sub>2</sub> (0.2 M), TFAA (1 equiv.) added, stirred 1 h; cooled to –78 °C, AlMe<sub>3</sub> (3 equiv.) and TMSOTf (1 equiv.) sequentially added, stirred 2 h; rt for 1 h.

<sup>i</sup>Crude in CH<sub>2</sub>Cl<sub>2</sub> (0.2 M), MsCl (1 equiv.) and Et<sub>3</sub>N (1 equiv.) added, stirred 1 h; washed NaHCO<sub>3</sub>, dried, reduced; redissolved in CH<sub>2</sub>Cl<sub>2</sub>, AlMe<sub>3</sub> (3 equiv.) added at –78 °C, stirred 2 h; rt for 1 h.

<sup>j</sup>MeMgBr (3 equiv.) added at –78 °C, stirred 3 h.

<sup>k</sup>Yield by crude <sup>1</sup>H NMR.

## Supplementary Material

Refer to Web version on PubMed Central for supplementary material.

## Acknowledgments

Financial support for this work was provided by the NIGMS Maximizing Investigators' Research Award MIRA (R35 GM122525) and support from Pfizer to study the modifications of natural products and medicinal compounds. We thank Dr. L. Zhu and the SCS NMR Lab for assistance with nuclear magnetic resonance spectroscopy and B. Budaitis for checking the procedure in Figure 3, 8. The Bruker 500-Mz NMR spectrometer was obtained with the financial support of the Roy J. Carver Charitable Trust, Muscatine, Iowa, USA. The data reported in this paper are tabulated in the Supplementary Information.

## References

- Schönherr H & Cernak T Profound methyl effects in drug discovery and a call for new C–H methylation reactions. *Angew. Chem. Int. Ed* 52, 12256–12267 (2013).
- Cernak T, Dykstra KD, Tyagarajan S, Vachal P & Krska SW The medicinal chemist's toolbox for late stage functionalization of drug-like molecules. *Chem. Soc. Rev* 45, 546–576 (2016). [PubMed: 26507237]
- Barreiro EJ, Kümmerle AE & Fraga CAM The methylation effect in medicinal chemistry. *Chem. Rev*, 111, 5215–5246 (2011). [PubMed: 21631125]
- Leung CS, Leung SSF, Tirado-Rives J & Jorgensen WL Methyl effects on protein-ligand binding. *J. Med. Chem* 55, 4489–4500 (2012). [PubMed: 22500930]
- Fauber BP et al. Discovery of 1-[4-[3-Fluoro-4-((3S,6R)-3-methyl-1,1-dioxo-6-phenyl-[1,2]thiazinan-2-ylmethyl)-phenyl]-piperazin-1-yl]-ethanone (GNE-3500): a potent, selective, and orally bioavailable retinoic acid receptor-related orphan receptor c (RORc or ROR $\gamma$ ) inverse agonist. *J. Med. Chem* 58, 5308–5322 (2015). [PubMed: 26061388]
- Quancard J et al. A potent and selective S1P<sub>1</sub> antagonist with efficacy in experimental autoimmune encephalomyelitis. *Chem. Biol* 19, 1142–1151 (2012). [PubMed: 22999882]
- Belshaw PJ, Schoepfer JG, Liu K-Q, Morrison KL & Schreiber SL Rational design of orthogonal receptor-ligand combinations. *Angew. Chem. Int. Ed* 34, 2129–2132 (1995).
- Shogren-Knaak MA, Alaimo PJ & Shokat KM Recent advances in chemical approaches to the study of biological systems. *Annu. Rev. Cell Dev. Biol* 17, 405–433 (2001). [PubMed: 11687495]
- Blakemore DC et al. Organic synthesis provides opportunities to transform drug discovery. *Nat. Chem* 10, 383–394 (2018). [PubMed: 29568051]
- White MC & Zhao J Aliphatic C–H oxidations for late-stage functionalization. *J. Am. Chem. Soc* 140, 13988–14009 (2018). [PubMed: 30185033]
- Campos KR Direct sp<sup>3</sup> C–H bond activation adjacent to nitrogen in heterocycles. *Chem. Soc. Rev* 36, 1069–1084 (2007). [PubMed: 17576475]
- Cordier CJ, Lundgren RJ & Fu GC Enantioconvergent cross-couplings of racemic alkylmetal reagents with unactivated secondary alkyl electrophiles: catalytic asymmetric Negishi  $\alpha$ -alkylations of *N*-Boc-pyrrolidine. *J. Am. Chem. Soc* 135, 10946–10949 (2013). [PubMed: 23869442]

13. Beak P, Basu A, Gallagher DJ, Park YS & Thayumanavan S Regioselective, diastereoselective, and enantioselective lithiation-substitution sequences: reaction pathways and synthetic applications. *Acc. Chem. Res* 29, 552–560. (1996)
14. Milligan JA, Phelan JP, Badir SO & Molander GA Alkyl carbon-carbon bond formation by nickel/photoredox cross-coupling. *Angew. Chem. Int. Ed* 58, 6152–6163 (2019).
15. Paul A & Seidel D  $\alpha$ -Functionalization of cyclic secondary amines: Lewis acid promoted addition of organometallics to transient imines. *J. Am. Chem. Soc* 141, 8778–8782 (2019). [PubMed: 31117670]
16. Jain P, Verma P, Xia G & Yu J-Q Enantioselective amine  $\alpha$ -functionalization via palladium-catalysed C–H arylation of thioamides. *Nat. Chem* 9, 140–144 (2017). [PubMed: 28282045]
17. Le C, Liang Y, Evans RW, Li X & MacMillan DWC Selective  $sp^3$  C–H alkylation via polarity-match-based cross-coupling. *Nature* 547, 79–83 (2017). [PubMed: 28636596]
18. Hiemstra H & Speckamp WN “Additions to *N*-acyliminium ions” in *Comprehensive Organic Synthesis: Selectivity, Strategy & Efficiency in Modern Organic Chemistry*, Trost BM. & Fleming I. (Pergamon Press, 2007), vol. 2, “Additions to C–X  $\pi$  bonds part 2”, chap. 4.5.
19. Andrus MB & Lashley JC Copper catalyzed allylic oxidation with peresters. *Tetrahedron*, 58, 845–866 (2002).
20. Li Z, Bohle DS & Li C-J Cu-catalyzed cross-dehydrogenative coupling : a versatile strategy for C–C bond formations via the oxidative activation of  $sp^3$  C–H bonds. *PNAS*, 103, 8928–8933 (2006). [PubMed: 16754869]
21. Kato N, Hamaguchi Y, Umezawa N & Higuchi T Efficient oxidation of ethers with pyridine *N*-oxide catalyzed by ruthenium porphyrins. *J. Porphyr. Phthalocyanines* 19, 411–416 (2015).
22. Ito R, Umezawa N & Higuchi T Unique oxidation reaction of amides with pyridine-*N*-oxide catalyzed by ruthenium porphyrin: direct oxidative conversion of *N*-acyl-L-proline to *N*-acyl-L-glutamate. *J. Am. Chem. Soc* 127, 834–835 (2005). [PubMed: 15656611]
23. Yoshifuji S, Tanaka K-I, Kawai T & Nitta Y Chemical conversion of cyclic  $\alpha$ -amino acids to  $\alpha$ -aminodicarboxylic acids by improved ruthenium tetroxide oxidation. *Chem. Pharm. Bull* 33, 5515–5521 (1985).
24. Kawamata Y et al. Scalable, electrochemical oxidation of unactivated C–H bonds. *J. Am. Chem. Soc* 139, 7448–7451 (2017). [PubMed: 28510449]
25. Annese C, D’Accolti L, Fusco C, Licini G & Zonta C Heterolytic (2e) vs homolytic (1e) oxidation reactivity: N–H versus C–H switch in the oxidation of lactams by dioxirans. *Chem. Eur. J* 23, 259–262 (2017). [PubMed: 27779338]
26. Cui L; Peng Y & Zhang L A two-step, formal [4+2] approach toward piperidin-4-ones via au catalysis. *J. Am. Chem. Soc* 2009, 131, 8394–8395. [PubMed: 19492799]
27. Zhao J, Nanjo T, de Lucca EC & White MC Chemoselective methylene oxidation in aromatic molecules. *Nat. Chem* 11, 213–221 (2019). [PubMed: 30559371]
28. Chen MS & White MC Combined effects on selectivity in Fe-catalyzed methylene oxidation. *Science*, 327, 566–571 (2010). [PubMed: 20110502]
29. Gormisky PE & White MC Catalyst-controlled aliphatic C–H oxidations with a predictive model for site-selectivity. *J. Am. Chem. Soc* 135, 14052–14055 (2013). [PubMed: 24020940]
30. Osberger TJ, Rogness DC, Kohrt JT, Stepan AF & White MC Oxidative diversification of amino acids and peptides by small-molecule iron catalysis. *Nature* 537, 214–219 (2016). [PubMed: 27479323]
31. Milan M, Carboni G, Salamone M, Costas M & Bietti M Tuning selectivity in aliphatic C–H bond oxidation of *N*-alkylamides and phthalimides catalyzed by manganese complexes. *ACS Catal.* 7, 5903–5911 (2017).
32. Nicolaou KC, Dolle RE, Chucholowski A & Randall JL Reactions of glycosyl fluorides. Synthesis of *C*-glycosides. *J. Chem. Soc. Chem. Commun* 1153–1154 (1984).
33. Posner GH & Haines SR Conversion of glycosyl fluorides into *c*-glycosides using organoaluminum reagents. Stereospecific alkylation at C-6 of a pyranose sugar. *Tetrahedron Lett.* 26, 1823–1826 (1985).
34. Mason JD & Weinreb SM Total syntheses of the monoterpene indole alkaloids ( $\pm$ )-alstoscholarisine B and C. *Angew. Chem. Int. Ed* 56, 16674–16676 (2017).

35. Taylor RD, MacCoss M & Lawson ADG Rings in drugs. *J. Med. Chem* 57, 5845–5859 (2014). [PubMed: 24471928]
36. Vitaku E, Smith DT & Njardarson JT Analysis of the structural diversity, substitution patterns, and frequency of nitrogen heterocycles among U.S. FDA approved pharmaceuticals. *J. Med. Chem* 57, 10257–10274 (2014). [PubMed: 25255204]
37. Stevens RV Nucleophilic additions to tetrahydropyridinium salts. Applications to alkaloid syntheses. *Acc. Chem. Res* 17, 289–296 (1984).
38. Tomooka K, Matsuzawa K, Suzuki K & Tsuchihashi G.-i. Lactols in stereoselection 2. Stereoselective synthesis of disubstituted cyclic ethers. *Tetrahedron Lett.* 28, 6339–6342 (1987).
39. Lunn MR et al. Indoprofen upregulates the survival motor neuron protein through a cyclooxygenase-independent mechanism. *Chem. Biol* 11, 1489–1493 (2004). [PubMed: 15555999]
40. Howell JM, Feng K, Clark JR, Trzepkowski LJ & White MC Remote oxidation of aliphatic C–H bonds in nitrogen-containing molecules. *J. Am. Chem. Soc* 137, 14590–14593 (2015). [PubMed: 26536374]
41. Prendergast MA et al. Central nicotinic receptor agonists ABT-418, ABT-089, and (–)-nicotine reduce distractibility in adult monkeys. *Psychopharmacology* 136, 50–58 (1998). [PubMed: 9537682]
42. Maryanoff BE et al. Pyrroloisoquinoline antidepressants. Potent, enantioselective inhibition of tetrabenazine-induced ptosis and neuronal uptake of norepinephrine, dopamine, and serotonin. *J. Med. Chem* 27, 943–946 (1984). [PubMed: 6747993]
43. Sugi K et al. Improved synthesis of paroxetine hydrochloride propan-2-ol solvate through one of metabolites in humans, and characterization of the solvate crystals. *Chem. Pharm. Bull.* 48, 529–536 (2000).
44. Fujimoto J et al. Discovery of 3,5-diphenyl-4-methyl-1,3-oxazolidin-2-ones as novel, potent, and orally available  $\Delta^5$  desaturase (D5D) inhibitors. *J. Med. Chem* 60, 8963–8981 (2017). [PubMed: 29023121]
45. Kitamura M, Ohmori K & Suzuki K Divergent behavior of cobalt-complexed enyne having a leaving group. *Tetrahedron Lett.* 40, 4563–4566 (1999).

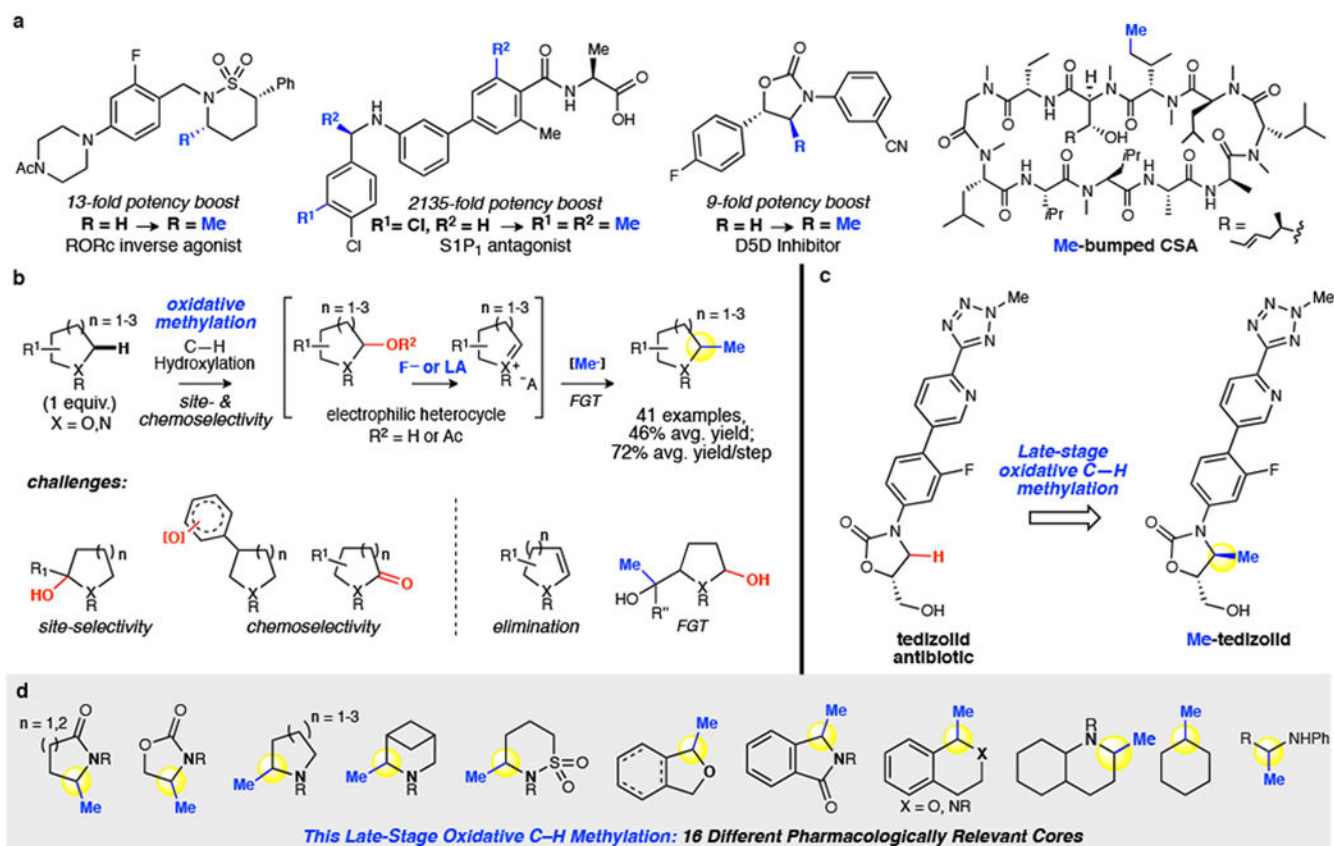


**Fig. 1 | C(sp<sup>3</sup>)-H methylation.**

**a**, The magic methyl effect boosts potency of drugs and furnishes biological probes. **b**, This oxidative methylation proceeds through an electrophilic intermediate. Challenges included over-oxidation, unselective oxidation, elimination and unselective methylation pathways. **c**, Late stage oxidative methylation of antibiotic tedizolid. **d**, Oxidative C-H methylation is demonstrated on 16 different pharmaceutically relevant cores. Using only 1 equivalent of substrate, methylation proceeds site-selectively and with functional group tolerance to afford preparative yields in 41 examples (including 18 complex bioactive molecules).

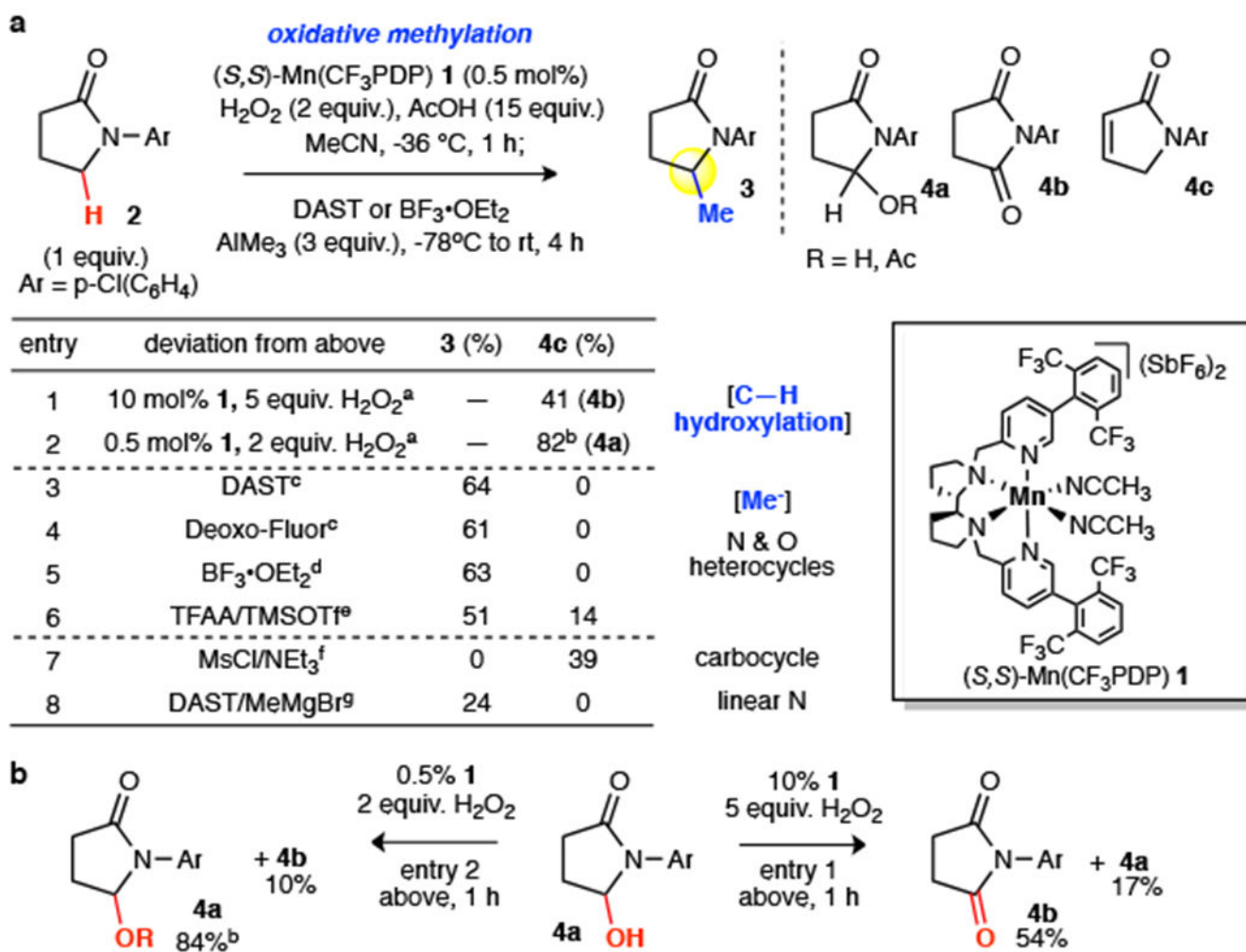


**Fig. 2 |. Reaction development.**

**a**, Optimization of the oxidative methylation reaction. For achiral substrates, (*R,R*)- and (*S,S*)-**1** can be used interchangeably. **b**, Exposure of hemiaminal to mild C–H hydroxylation developed here (0.5 mol% **1**, 2 equiv. H<sub>2</sub>O<sub>2</sub>) gives little overoxidation to the imide. The previous forcing condition (10 mol% **1**, 5 equiv. H<sub>2</sub>O<sub>2</sub>) results in imide as the major product. <sup>a</sup>No methylation. <sup>b</sup>Mixture of hemiaminal (64%–71%) and hemiaminal acetate from AcOH (13%–18%). <sup>c</sup>1 equiv. <sup>d</sup>2 equiv. <sup>e</sup>TFAA (1 equiv.), TMSOTf (1 equiv.). <sup>f</sup>MsCl (1 equiv.), NEt<sub>3</sub> (1 equiv.), NaHCO<sub>3</sub> wash; AlMe<sub>3</sub> (3 equiv.), –78 °C, 2 h; rt 1 h. <sup>g</sup>MeMgBr (3 equiv.), –78 °C, 3 h.

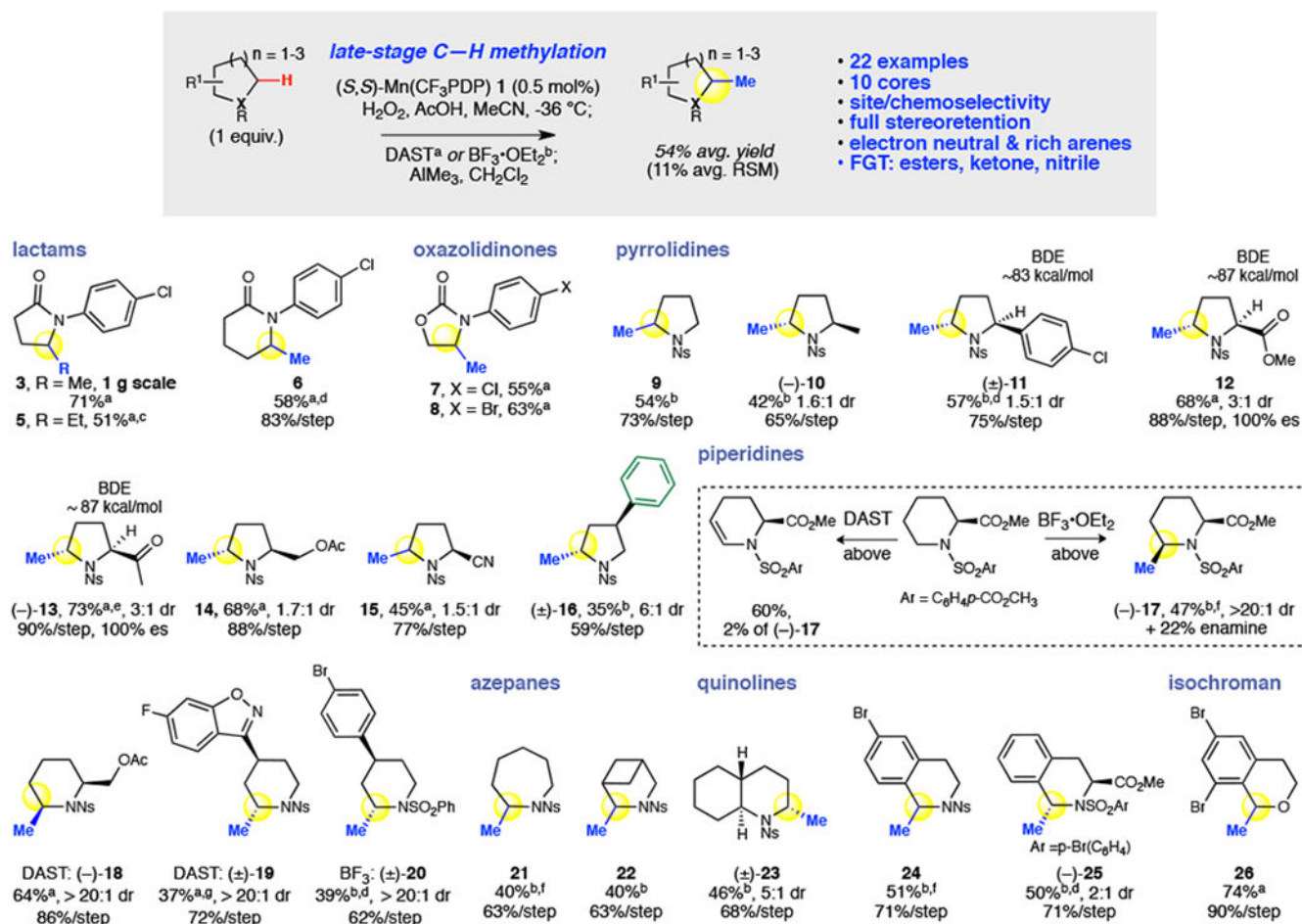


**Fig. 3 | Ten different heterocyclic cores, commonly found in pharmaceuticals, were explored in the  $\text{Mn}(\text{CF}_3\text{PDP}) \textbf{1}$ -catalyzed C–H hydroxylation and methylation.**

Twenty-two heterocycles including lactams, oxazolidinones, pyrrolidines, piperidines, azepane, azabicycloheptane, quinolines, and isochroman were oxidatively methylated in preparative overall yields (54% average) using limiting substrate. General oxidation: substrate, catalyst (0.5 mol%), AcOH in MeCN,  $-36^\circ\text{C}$ ;  $\text{H}_2\text{O}_2$  (2 or 5 equiv.) in MeCN syringe pump 1 h. Mixture passed through silica plug, EtOAc flush, concentrated prior to isolation or methylation. For insoluble substrates,  $\text{CH}_2\text{Cl}_2$  added to MeCN and/or  $0^\circ\text{C}$ .

<sup>a</sup>DAST Activation: crude in  $\text{CH}_2\text{Cl}_2$  (0.2 M), DAST (1 equiv.) added at  $-78^\circ\text{C}$ ; room temperature (rt) for 1 h; cooled to  $-78^\circ\text{C}$ ,  $\text{AlMe}_3$  added, stirred 2 h; rt for 1 h. <sup>b</sup> $\text{BF}_3$  Activation: crude in  $\text{CH}_2\text{Cl}_2$  (0.2 M),  $-78^\circ\text{C}$ ,  $\text{AlMe}_3$  (3 equiv.) and  $\text{BF}_3\cdot\text{OEt}_2$  (2 equiv.) sequentially added, stirred 1 h; rt for 3 h. <sup>c</sup>Triethylaluminum. <sup>d</sup>2 mol% (*S,S*)-**1**. <sup>e</sup> $\text{AlMe}_3$   $-78^\circ\text{C}$ , 3 h. <sup>f</sup>1 mol% (*S,S*)-**1**. <sup>g</sup>For facile purification, hemiaminal isolated before methylation. 10 mol% (*S,S*)-**1**, rt, starting material recycled 1x.

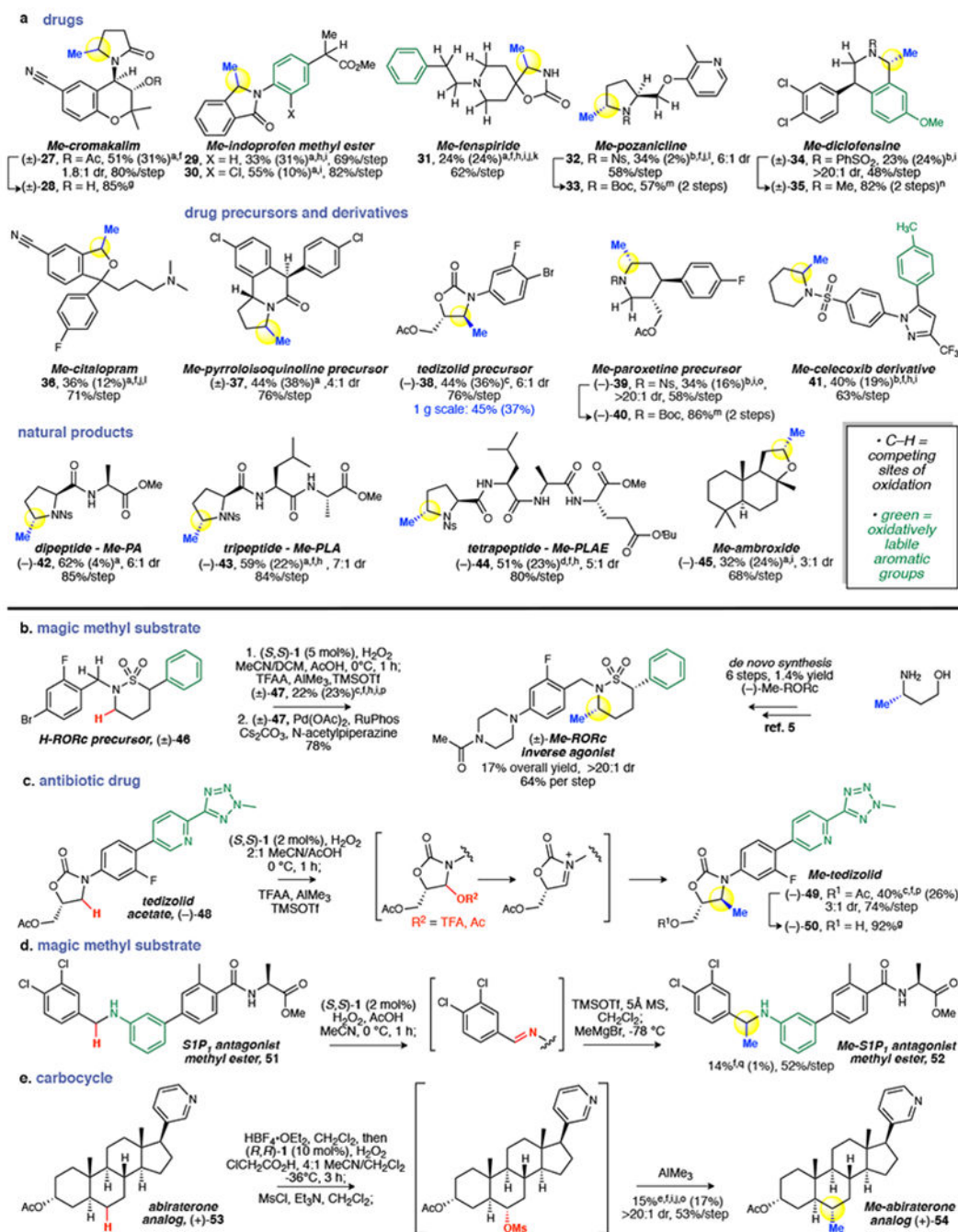


**Fig. 4 | Application of oxidative methylation for late stage functionalization.**

**a.** Selective methylation of drugs, drug precursors, intermediates and natural products underscores the power of this method for late stage applications. Generally, 0.5 to 5 mol% (S,S)-1 and 2 or 5 equiv. H<sub>2</sub>O<sub>2</sub> were used for oxidation. Higher catalyst and oxidant loadings were applied when conversions were low. **b.** Methylation of an RORc inverse agonist precursor rapidly furnishes the analogue with 13-fold potency boost. **c.** Methylation of antibiotic tedizolid acetate furnishes Me-tedizolid. **d.** Methylation of linear aniline in S1P<sub>1</sub> antagonist methyl ester occurs at a position where magic methyl effect was observed to

contribute to a 2135-fold potency boost. **e**, Remote methylation of a carbocycle on an abiraterone analog. <sup>a</sup>DAST activation. <sup>b</sup>BF<sub>3</sub> activation. <sup>c</sup>TMSOTf activation: TFAA, rt, 1 h; cooled to -78 °C, AlMe<sub>3</sub> and TMSOTf sequentially added, 2 h; then rt, 1 h. <sup>d</sup>Deoxo-Fluor activation. <sup>e</sup>Mesylation activation: MsCl and Et<sub>3</sub>N added, rt, 1 h; NaHCO<sub>3</sub> wash, dried, condensed; redissolved in CH<sub>2</sub>Cl<sub>2</sub>, AlMe<sub>3</sub> added at -78 °C, stirred 2 h; then rt, 1 h. <sup>f</sup>Oxidation intermediates isolated before methylation. <sup>g</sup>1 M NaOH/MeOH. <sup>h</sup>Starting material recycled 1x. <sup>i</sup>For insoluble substrates, CH<sub>2</sub>Cl<sub>2</sub> added to MeCN and/or 0 °C. <sup>j</sup>HBF<sub>4</sub> protection, ref. 40. <sup>k</sup>10 mol% (*S,S*)-Mn(PDP)(SbF<sub>6</sub>)<sub>2</sub>. <sup>l</sup>10 mol% (*S,S*)-**1**. <sup>m</sup>PhSH, Cs<sub>2</sub>CO<sub>3</sub>; Boc<sub>2</sub>O. <sup>n</sup>Mg, NH<sub>4</sub>Cl; formaldehyde, formic acid. <sup>o</sup>10 mol% (*RR*)-**1**. <sup>p</sup>2 equiv. TMSOTf. <sup>q</sup>TMSOTf (1.2 equiv.), 0 °C, 1 h, then MeMgBr (3.0 equiv.) -78 °C, 4 h, repeated once.